lubricants

MDPI

Article

The Effect of Agglomeration Reduction on the Tribological Behavior of WS_2 and MoS_2 Nanoparticle Additives in the Boundary Lubrication Regime

Yosef Jazaa, Tian Lan, Sonal Padalkar and Sriram Sundararajan *

Department of Mechanical Engineering, Iowa State University, Ames, IA 50011, USA; yajazaa@jazanu.edu.sa (Y.J.); tlan@iastate.edu (T.L.); padalkar@iastate.edu (S.P.)

* Correspondence: srirams@iastate.edu; Tel.: +515-294-1050

Received: 7 August 2018; Accepted: 28 November 2018; Published: 10 December 2018

Abstract: This study investigates the impact of different surfactants and dispersion techniques on the friction and wear behavior of WS_2 and MoS_2 nanoparticles additives in a Polyalphaolefin (PAO) base oil under boundary lubrication conditions. The nanoparticles were dispersed using Oleic acid (OA) and Polyvinylpyrrolidone (PVP) to investigate their impact on particle agglomeration. The size distribution of the dispersed nanoparticles in PAO was measured by dynamic light scattering. The nanoparticles treated using PVP resulted in the most stable particle size. Friction studies showed that nanoparticle agglomeration reduction and the homogeneity of the suspension did not significantly impact the friction reduction behavior of the lubricant. Reciprocating wear experiments showed that, for our test conditions, both WS_2 and MoS_2 nano additives exhibited maximum wear depth reduction (45%) when using the PVP surface treatment compared to base oil. The wear results confirmed the significance of minimizing agglomeration and promoting high dispersion in promoting favorable wear resistance under boundary lubricant conditions. Analysis of the wear surfaces showed that a tribofilm formation was the primary wear reduction mechanism for WS_2 particles treated by PVP while, in the case of MoS_2 treated by PVP, the mechanism was load sharing via particles rolling and/or sliding at the interface.

Keywords: nanoparticles; agglomeration; lubricant additives; boundary lubrication; sliding wear

1. Introduction

Several studies have shown that tribological behavior of a lubricant can be improved by dispersing a small amount of nanomaterials in base oil. Dispersing nanoparticles in lubricant is a challenging process since the particles tend to agglomerate due to strong Van der Waal forces [1–3]. The literature shows that dispersion of nanoparticles additives can be improved by using a number of techniques including sonicating, which includes both bath or probe sonication, adding a surfactant, or a combination of the previously mentioned techniques [3–11]. Specifics of the dispersion method is dictated by the nanoparticles and their surface energy [3,12].

In this study, we selected two dichalcogenides nanoparticles known as WS_2 and MoS_2 that have been shown to improve tribological behavior as additives. The use of MoS_2 nanoparticles has been extensively investigated over the last several years. Multiple studies on MoS_2 nanoparticles did not use a surfactant to stabilize the nanoparticles when added to the lubricant [13–18]. However, MoS_2 nanoparticles have a strong tendency to agglomerate when added to lubricants [18–20]. Other studies investigated the dispersion of the MoS_2 nanoparticles and showed that the agglomeration could be reduced by adding surfactant via bath sonication [21–23]. Similarly, there are studies that have demonstrated improved tribological behavior using WS_2 nanoparticle additives with Refs. [16,24–30]

and without Refs. [22,23,31–34] as well as the use of surfactants. Nevertheless, these results suggest there is a need to determine if reduced agglomeration and dispersion stability directly contribute to improving tribological performance.

The present paper investigates the impact of different surfactants and dispersion techniques on the friction and wear behavior of WS_2 and MoS_2 nanoparticle additives in a Polyalphaolefin (PAO) base oil under boundary lubrication conditions. The substrate chosen was 8620 steel, which is used in drivetrain components in energy generation and agricultural machinery. Oleic acid (OA) and Polyvinylpyrrolidone (PVP) were chosen as surfactants. Both these materials are commonly used in the literature to stabilize nanomaterials additives [7,35–39]. Our initial work showed that, while OA was effective in reducing agglomeration for CuO and WC nanoparticle additives, they were less effective for WS_2 particles. PVP has been shown to be effective for dichalcogenides due to reducing repulsive forces between its hydrophobic chains [22,23,40].

2. Materials and Methods

2.1. Materials

The neat base oil used in this experiment was Polyalphaolefin (PAO) with the following specifications, as reported by the manufacturer (Exxon Mobile Corporation, Spring, TX, USA): density 826 g/m^3 at 15 °C and viscosity 400 cSt at 40 °C. WS_2 nanoparticles were purchased commercially (Zhengzhou Dongyao Nano Materials Co., Ltd., Zhengzhou, China) and had the following properties: a spherical shape with a nominal diameter of 100 (nm), density of 7.5 (g/m^3), and a hardness of 0.75 (mhos). MoS_2 nanoparticles were synthesized using a hydrothermal process and were described as follows. First, separate aqueous solutions of (7 mM) ammonium molybdate tetrahydrate ($(NH_4)_6Mo_7O_{24}\cdot 4H_2O$; 99.98%) and (35 mM) thiourea (Both purchased from Sigma-Aldrich, St. Louis, Mo, USA) were prepared. Next, the solutions were mixed together to obtain a total volume of 50 mL. The final solution was vigorously stirred for 20 min before it was transferred to a Teflon-lined stainless-steel autoclave. The hydrothermal process was carried out at 180 °C for 15 h after which the autoclave was cooled to room temperature and the black powder of MoS_2 was collected. The MoS_2 powder was centrifuged and washed three times with deionized water and ethanol. The powder was dried at 60 °C for 2 h. The MoS_2 nanoparticles prepared had the following properties: a spherical shape with a nominal diameter of 100 (nm), density of 5.06 (g/m^3), and a hardness of 1.5 (mhos).

The surfactants used in this study were Oleic acid and Polyvinylpyrrolidone (both purchased from Sigma-Aldrich). Oleic acid is a surfactant containing a hydrophilic hydroxyl end group and an organophilic alkyl chain [4]. PVP is a non-ionic polymer that contains a strong hydrophilic molecule that can attach easily to materials in the solution [36]. Figure 1 shows a schematic for the chemical structure of OA and PVP.

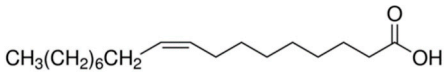

Oleic acid (OA)

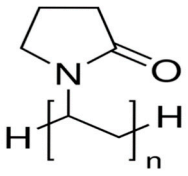

Polyvinylpyrrolidone (PVP)

Figure 1. Schematic of the chemical structures of Oleic acid (OA) and Polyvinylpyrrolidone (PVP) that were chosen as surfactants.

In this study, the concentration of the nanoparticle additives in oil was chosen to be 1% by weight for each nanoparticle sample based on the recommendation from studies on a variety of material additives [26,30,41–43]. The particles added without any surfactant were sonicated for 60 min. For the formulations using Oleic acid as a surfactant, the samples were prepared by mixing 1% of weight Oleic acid to the PAO 1 wt % nanoparticle solutions and sonicating the particles for 120 min. For the formulations using PVP as a surfactant, the samples were prepared as follows. Nanoparticles and PVP were added to the distilled water in the ratio of 3:1 by weight. The solution was subsequently sonicated for 30 min, which is followed by drying in an oven at 60 °C for two hours. The resulting dry nanoparticles were added to the oil and sonicated for 60 min using Cole-Pramer Ultrasonic Bath (Cole-Pramer, Vernon Hills, IL, USA, 115 VAC, 0.8 amps, and High-frequency 42 kHz, at 40 °C).

2.2. Methods

2.2.1. Dynamic Light Scattering

Extant research demonstrates that the agglomeration of nanoparticles tends to occur when they are added to oil [44]. Once agglomeration occurs, the particles size keeps changing. For a better estimate of the nominal particle size in the solution, the size distribution of dispersed nanoparticles in PAO was measured by dynamic light scattering (DLS) (Malvern ZetaSizer Nano ZS, Westborough, MA, USA). The theory underlying the measurements of the Zetasizer are based on effects of Brownian motions of nanoparticles on Rayleigh light scattering data to determine the size of a particle/molecule in the solution [45]. The primary result obtained from a DLS measurement represents the intensity-weighted mean diameter derived from the cumulants, which is very sensitive to the existence of nanoparticles agglomeration due to the inherent intensity weighting. Given that the typical friction and wear test time lasts for 60 min, the hydrodynamic diameter distribution of the particles in the solution was measured and collected four times at 15-minute intervals over the span of an hour and the corresponding data were recorded.

2.2.2. Friction and Wear Testing

For the friction and wear experiments, a custom-built reciprocating ball-on-flat micro-tribometer that can produce a microscale (apparent area ~1000 μm^2) multi-asperity contact was used [46]. A schematic of the micro-tribometer major components is shown in Figure 2. A probe with a specific radius is placed at the end of a crossed I-beam structure, which is lowered using a linear stage to apply a desired normal load to the sample. For this study, a SiC probe (4 mm diameter, hardness = 9 mohs, v = 0.19, E = 415 GPa) and an AISI 8620 steel substrate (4.5 mohs hardness, v = 0.29, E = 200 GPa) were used. The average substrate surface roughness (Ra) was approximately 0.06 µm as measured by a Zygo NewView (Zygo, Middlefield, CT, USA) 7100 non-contact profilometer over a scan area of 0.47 mm × 0.35 mm.

The normal and the friction (lateral) forces in the micro-tribometer are measured using semiconductor strain gages on the cantilevers. Friction forces can be resolved to approximately ±5 µN and normal forces to approximately ±15 µN. The signal from the normal load is monitored and used in a simple proportional-integral (PI) feedback loop to maintain the desired normal force regardless of any slope or waviness in the surface of the sample. The desired sample is affixed to another stage set perpendicular to the beam, which provides a linear motion. An appropriate amount of the formulated oil was dropped to a fresh substrate surface prior to conducting each test. A new SiC probe was used for each friction and wear test.

To evaluate the coefficient of friction, the applied normal load was increased linearly from 0 to 2000 mN for a specific sliding distance of 25 mm at a speed of 1 mm/s. To obtain the coefficient of friction, ramped load tests were performed in which the normal load increased linearly with the sliding distance while the friction force was monitored. The load was increased from 0.2 to 200 mN since the probe was moved across a stroke distance. Based on these parameters, the maximum Hertzian

contact pressure was estimated to be 1.27 GPa and the lubrication regime was boundary lubrication. The lateral force was recorded continuously along with the normal load for each test, which provides a coefficient of friction. Five replicates were conducted for each condition and the average coefficient of friction values were reported along with the 90% confidence interval. In order to obtain the wear response, a reciprocating sliding wear test was performed against the SiC probe at a constant load of 5400 mN (maximum Hertzian force of 1.77 GPa) for 200 cycles, a stroke length of 8 mm, and a stroke speed of 10 mm/s. Two replicates were conducted for each sample. After each test, the sample surface was cleaned with isopropyl alcohol wipes and the wear track depth was measured using the Zygo profilometer. An average wear depth was reported from five measurements along each wear track and the data was reported as an average of 10 measurements (from two tests) along with a 90% confidence interval. Note that the test condition consisting of base oil with no additives was used as a control.

An FEI Quanta-250 Scanning Electron Microscope (FESEM, Supra 400VP Gemini, Jena, Germany) was used to obtain high-resolution images of wear tracks (Oxford Aztec energy-dispersive X-ray analysis, Abingdon, UK) was used to perform point analysis of the wear track and adjacent regions for evidence of any tribo-film formation. Backscattered images were analyzed for further tribo-film analysis with an accelerating voltage of 10 kV and a spot size of 4 A.U. for all cases.

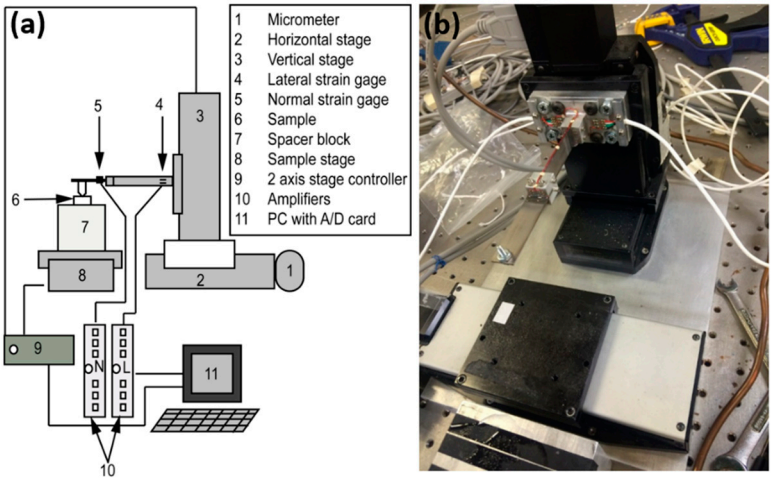

Figure 2. (**a**) Schematic of micro-tribometer used for friction and wear tests. (**b**) A photograph of the micro-tribometer.

3. Results

The results are presented and discussed in the following three sections. First, we describe the results related to reducing agglomeration of nanoparticle additives when dispersed in base oil. Next, we describe the friction behavior of the nano-additives, which is followed by the results of the stable nano-additives on wear behavior.

3.1. Dispersion of Nanoparticles in Oil

Figure 3 shows the average particle size as a function of post sonication time for the two nanoparticle additives and surfactants. The use of particles without surfactant resulted in an initially high particles size (350–420 nm) and a gradual decrease over the testing duration with sizes of about 200 nm at 60 min. However, the absence of surfactants did lead to a very high variability in the particle size, which suggests unstable dispersion. For both particles, dispersing with PVP provided the lowest and most stable particle size for the testing duration. The stable particle size was around 150 nm and 100 nm for WS_2 and MoS_2 nanoparticles during the testing duration used. OA was less effective in reducing agglomeration when compared to PVP and by the 60 min mark, which did not show appreciable improvements when compared to the condition without surfactant. OA as a surfactant was more effective in the case of MoS_2 with a particle size of 200 nm but not as effective as PVP. However,

the variability in the particle size was very high when compared to PVP. This variability was even more apparent in the case of WS_2.

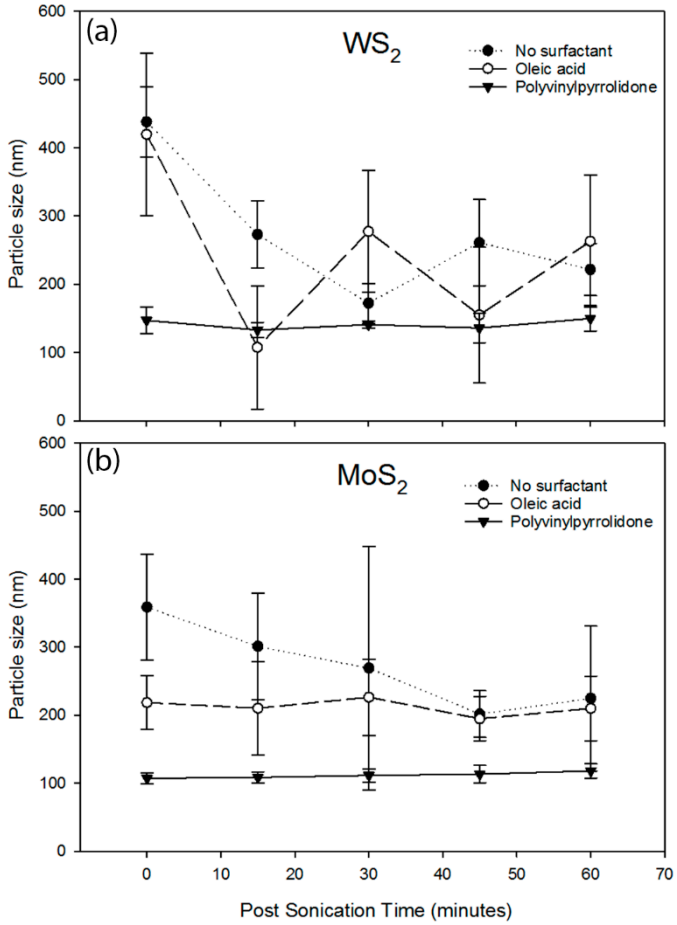

Figure 3. Dynamic light scattering (DLS) data show the average hydrodynamic diameter of (**a**) WS_2, (**b**) MoS_2, nanoparticles in PAO dispersed using different surfactants.

Overall, while the addition of Oleic acid as well as treating the nanoadditives by PVP can form a layer on the nanoparticle surface and contribute to an increased diameter, the data suggest that agglomeration is the greater contributor for the increased diameters observed. This is supported by the fact that the observed diameters for particles with surfactants were lower than that of particles without surfactant. Furthermore, despite the fact that the amount by weight of PVP in the oil formulations for both particles was less than that of oleic acid, the PVP dispersion technique showed a lower particle size, which points to agglomeration effects being the primary phenomenon captured by the DLS data. In addition, a visual impact confirmed that the dispersion did not settle, which eliminates this as a possible reason for observing a reduced particle size. Consequently, the dispersion technique using PVP contribute to effective agglomeration reduction and the most stable dispersion. We speculate that the difference in the chemical structure of the surfactants contributed to the difference in their impact on agglomeration. The hydrophobic chain interactions of PVP combined with its effectiveness in forming surface films appear to lead to lower surface energy when compared to the interactions of the non-polar ends of OA.

3.2. Friction Behavior

Figure 4 compares the reduction in the coefficient of friction observed for the formulations of nanoparticle additive samples relative to the coefficient of friction of the neat base oil (PAO). All formulations exhibited a friction reduction with reductions ranging from 12% to 33%.

When compared to the base oil, the average reduction using WS_2 particles with no surfactants was 25%. Additionally, the addition of oleic acid showed a 29% reduction while there was a 33% reduction using the PVP treatment for the WS_2 particles. There were high amounts of variability in friction reduction across the dispersion methods for WS_2, which suggests that the observed reductions are comparable among dispersion conditions even though the average reduction in friction using the PVP treatment was the highest. As such, it appears that agglomeration reduction of the WS_2 nanoparticles can result in improved friction performance under the specified testing conditions.

Friction tests of oil samples containing MoS_2 nano additives in base oil demonstrated lower levels of friction reduction when compared to WS_2. The measured average reduction percentage using MoS_2 added to the lubricant without surfactant was 25%. In addition, the oleic acid technique showed a 12% reduction on average while there was a 16% reduction using the PVP treatment. MoS_2 nanoparticles dispersed in lubricant without surfactant had the best friction reduction when compared to the other two techniques. The data indicates that agglomeration reduction of MoS_2 nanoparticle additives was not a requirement for effective friction reduction.

Overall, the nano-additives in this study reduced the coefficient of friction when compared to the neat base oil. These results suggest that the WS_2 particles reduce friction by providing avenues for rolling friction rather than sliding friction. Reduced agglomeration (using PVP) enhances the ball bearing effect, which provides lower friction when compared to conditions where agglomeration occurs (no surfactant). In contrast, for the MoS_2 nanoparticles, the primary mechanism is still the traditional shearing of planes, which explains why the occurrence of agglomeration has a better friction reduction when compared to the presence of individual particles [47]. The availability of more particles in the contact facilitate the shearing of the particles. It must be noted that intrinsic properties of the nanoparticles including the structure, the number of layers, and the defect may also influence their friction response.

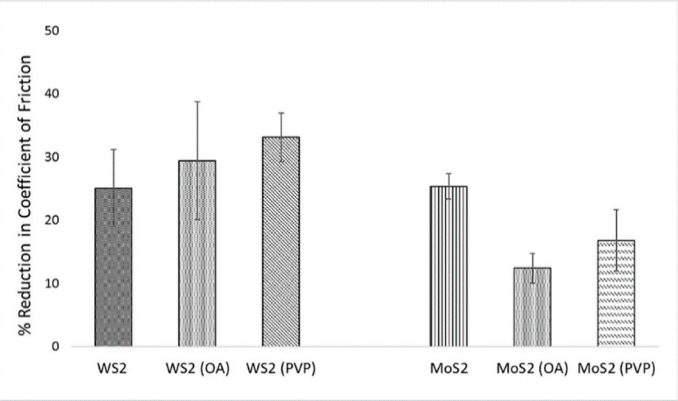

Figure 4. A comparison of the reduction in the coefficient of friction exhibited by the various dispersion techniques for WS_2 and MoS_2 nanoparticles. Reductions are expressed as percentages with respect to the coefficient of friction observed in a base oil condition. Average values are shown along with 90% confidence intervals.

3.3. Wear Behavior

Figure 5 shows the results of the wear tests using WS_2 and MoS_2 nano additives and different dispersion techniques. The results shown are reductions in wear scar depths for each formulation compared to the wear depth observed when using base oil. Positive values indicate improved wear performance while negative values indicate worse performance when compared to the wear depth observed with the base oil only. The changes on the wear behavior varied from −22% to +45%, which indicates that the nano additives could lead to an increase or decrease in the wear scar depth when compared to the base oil depending on the nanomaterial and the dispersion method

used. Figure 6 shows representative wear scar particles for the various nanomaterial additives and dispersion conditions.

WS_2 nanoparticles exhibited a relative wear reduction in all of the tested dispersion techniques. For example, when compared to the base oil, the average reduction percentage observed using no surfactants was 9%. Treatment with oleic acid yielded a 15% wear reduction while treatment with PVP resulted in a 43% reduction. When taken together with the DLS data in Figure 3a, these results show that reducing agglomeration and enhancing dispersion stability promoted increased wear resistance in terms of WS_2 nanoparticles.

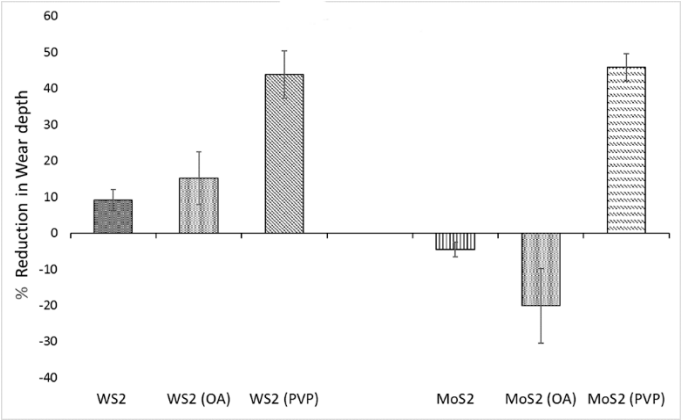

Figure 5. A comparison of the reduction in wear exhibited by the various dispersion techniques for WS_2 and MoS_2 nanoparticles. Reductions are expressed as percentages with respect to the wear observed with only the base oil. Positive values indicate improved wear performance while negative values indicate worse performance. Average values are shown along with 90% confidence intervals.

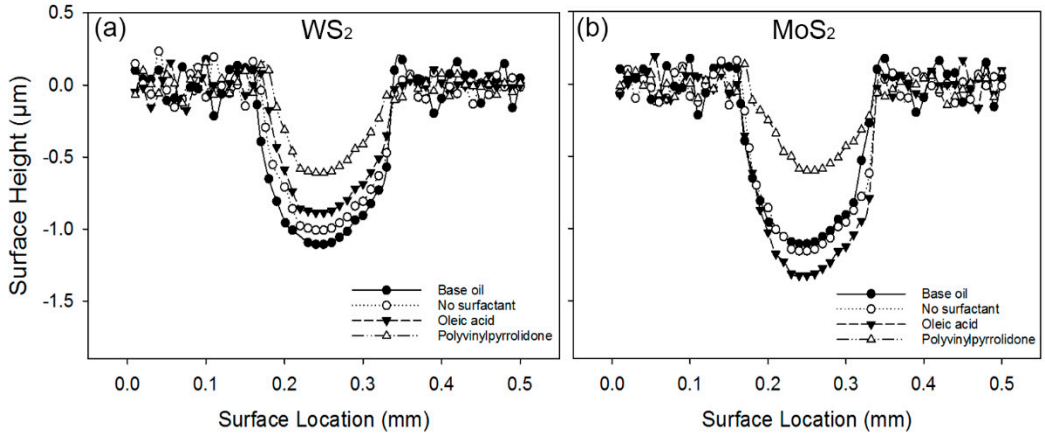

Figure 6. Representative wear scar profiles for (**a**) WS_2 nanoparticles and (**b**) MoS_2 nanoparticles with different surfactants, compared to the results for the base oil.

The MoS_2 nano-additives in base oil demonstrated different wear behavior than that of WS_2. The average wear reduction for MoS_2 when added to lubricant without surfactant was approximately −5%, which means that the wear scar depth increased by 5% when MoS_2 was added to the base oil. In addition, treatment with oleic acid increased wear depth by 20% when compared with the base oil. In contrast, the treatment with PVP, which is shown in Figure 3b, had the lowest and most stable particle size, which resulted in a 45% wear scar depth reduction when compared with base oil. This result suggests that agglomeration reduction of the nano-additives alleviate the wear resistance of the lubricant.

A primary interpretation of the nano additives behavior in boundary lubrication is that the small particles fill the valleys of the surface asperities and increases the real contact area. The nano

additives then help share the load subjected to the surface asperities and reduce wear. We investigated substrate surfaces lubricated with nanoparticles treated by PVP and without surfactant to better identify the prevailing mechanism of wear reduction. Figure 7 shows representative SEM images and EDS spectra of the wear tracks from the tests using the nanoparticles with and without PVP. Figure 7a shows the SEM image of the wear track of the surface lubricated with 1% WS_2 dispersed without surfactant. It demonstrates an existence of abrasive wear via plastic deformation that changed the surface topography of the wear track region. In contrast, Figure 7b demonstrates fewer changes in the surface topography inside the wear track when WS_2 nanoparticles were treated by PVP. Figure 7b also shows a lighter color inside the wear track, which suggests the existence of material layers other than steel. This layer could be debris from the contact surfaces or nano additives embedded in the surface. Figure 7c shows the chemical analysis of the unworn and worn surfaces for WS_2 additives with and without PVP. EDS data identified a higher peak intensity of W particles present inside the wear track when lubricated using WS_2 treated by PVP. However, no trace of sulfur was detected because the intensity line of sulfur is weaker. This supports nanoparticle-based film formation on the wear track surface that could be the cause of the higher wear reduction observed for this dispersion condition. It is also possible that PVP acts as a film promoter, but that mechanism needs further investigation.

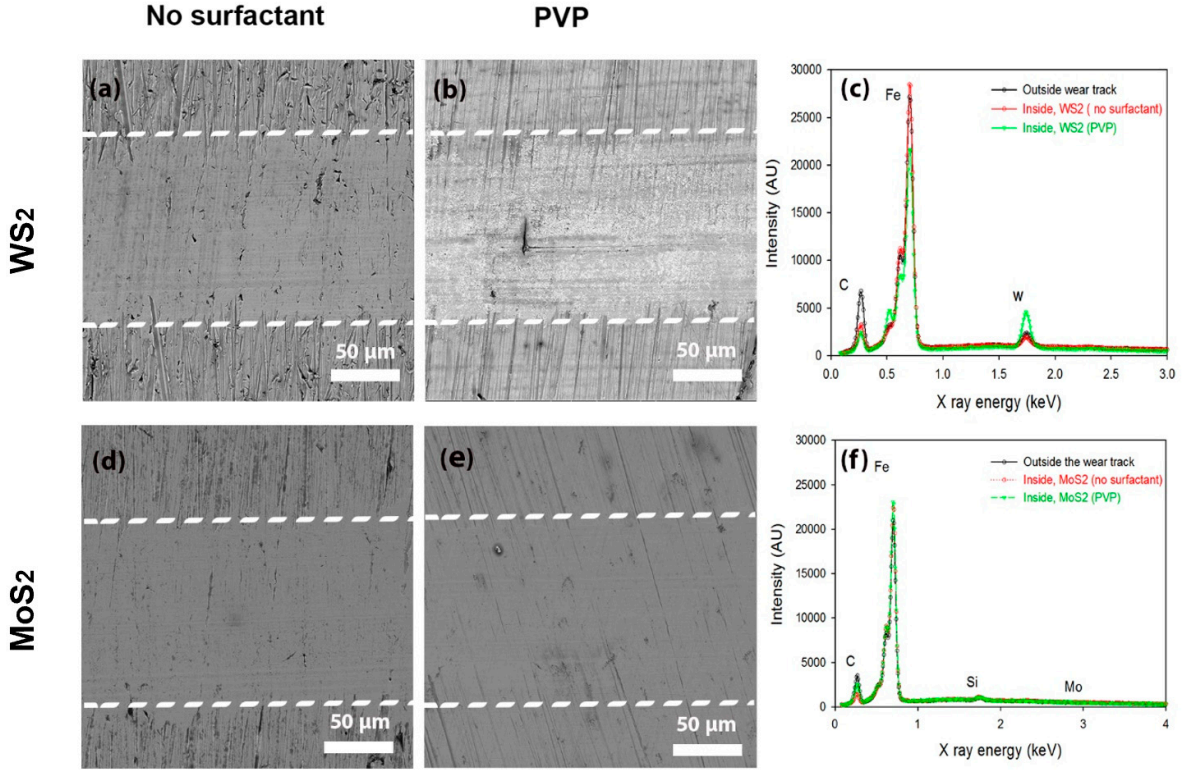

Figure 7. Scanning Electron Microscope (SEM) images of wear tracks on a steel substrate from sliding tests against a diamond probe of the wear track. (**a**) WS_2 as additives and (**b**) WS_2 treated by PVP. Dotted lines indicate the edges of the wear track. (**c**) EDS data for WS_2 nano additives from regions inside and outside the wear tracks. The figure demonstrates a lack of any particles or particle-based film formation when no surfactant used and adhered W materials to the surface forming a layer of particles or particle-based film when the additives treated by PVP. (**d**) MoS_2 as additives and (**e**) MoS_2 treated by PVP. (**f**) EDS data for the different MoS_2 nano additives from regions inside and outside the wear track show a lack of any particles or particle-based film formation.

Figure 7e,f compares MoS_2 nanoparticles dispersed with and without PVP. Wear tracks of the substrates show evidence of abrasive wear via ploughing, which is similar to that observed using WS_2. PVP treated nanoparticles resulted in less surface deformation on the worn surface and fewer changes on the surface topography between the outside and inside wear track regions. Analyses of SEM images

and EDS data for the substrates reveal no evidence of any MoS_2 nanoparticle-based material on any of the wear tracks. This suggests the mechanism of wear reduction for well-dispersed MoS_2 in the boundary lubrication condition, which is via load support of rolling nanoparticles rather than the formation of a tribo-film. The particles rolling mechanisms was also found in the literature as the dominant wear reduction [48–50]. The agglomeration reduction and homogeneous particle dispersion help to make particles roll more and contribute to the wear reduction.

We were expecting that WS_2 nanoparticles treated by PVP would provide a higher level of relative wear reduction compared to MoS_2 because of the tribo-film formed on the substrate. However, as demonstrated in Figure 4, the wear reduction in WS_2 was equivalent to MoS_2 nano additives treated by PVP, which we believe reduced wear via a nanoscale rolling effect. This equivalency may be due to the lack of durability of the WS_2, which is a tribo-film, or MoS_2, which may have formed a film as well but was removed before the 200 cycles were used in the previous analyses (Figure 5). In order to investigate these possibilities, we performed wear depth measurements and EDS analyses at 100, 200, 400, and 800 cycles at the same load. Figure 8a shows variations of the average wear scar depth as a function of sliding cycles. The wear scar depth increased sharply at first, but then gradually increased between 200 and 800 cycles. WS_2 showed a slightly lower wear rate increase when compared to MoS_2. At 800 cycles, WS_2 exhibited a slightly lower wear scar depth. However, this difference is minimal. Figure 8b shows EDS data for the wear tracks of various sliding cycles for WS_2 with PVP. A decrease in intensity of the adhered W materials to the surface is observed as the number of cycles increase. The data suggest that tribo-film formation is the dominant wear reduction mechanism when WS_2 with PVP is used. This tribo-film is susceptible to wear. This explains why it did not show higher relative wear reduction when compared with MoS_2 PVP. Despite the tribo-film wear susceptibility, it is quite durable under the tested conditions. Figure 8c shows the intensity level of Mo particles inside the wear track regions on the substrate surfaces when MoS_2 with PVP lubricated the particles for different wear track cycles. The data shows a lack of any particle or particle-based film formation when MoS_2 with PVP nano additives were used. The data reinforces the load sharing via rolling and that there was not any tribo-film formed under this condition.

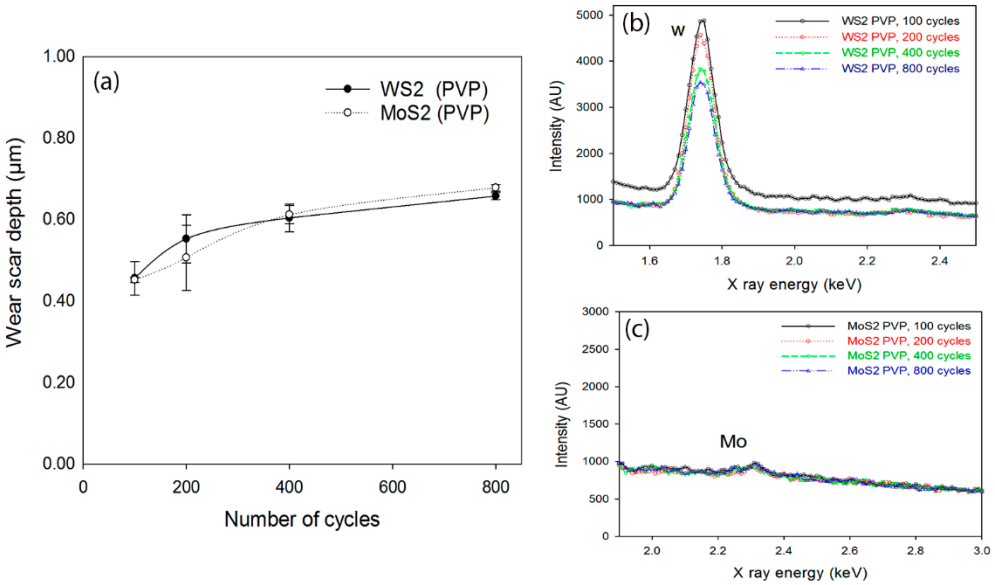

Figure 8. (**a**) Wear scar depth data in μm for different cycles when WS_2 and MoS_2 nanoparticles treated by PVP. (**b**) EDS data for WS_2 nano additives treated by PVP from regions inside the wear tracks for different cycles, which shows a decrease in the adhered W materials to the surface formed a layer of particles when the number of cycles increase. (**c**) EDS data for the MoS_2 nano additives treated by PVP from regions inside the wear tracks for different cycles shows a lack of any particle or particle-based film formation.

4. Conclusions

This study tested different suspension techniques for WS_2 and MoS_2 nanoparticles to enhance agglomeration reduction and improve the particle dispersion in PAO. Subsequently, the tribological behavior exhibited by the various dispersion techniques of the nanoparticles in a boundary lubricant regime was investigated. The nanoparticles were dispersed using the following techniques: (1) 60-minute sonication without using a stabilizing agent, (2) 60-minute sonication with 1% of weight oleic acid (OA), and (3) treating the nanoparticles using PVP (3:1 ratio of nanoparticles to PVP). The dispersion conditions using PVP showed the most stable particle size and homogeneous mixture dispersion for both nanoparticles.

Friction studies showed that nanoparticle agglomeration reduction and the homogeneity of the suspension did not significantly impact the friction reduction behavior of the lubricant. Reciprocating wear experiments showed that, for our test conditions, both WS_2 and MoS_2 nano additives showed maximum wear depth reduction (45%) when using the PVP surface treatment when compared to base oil. The wear results confirmed the significance of minimizing agglomeration, promoting high dispersion, and enabling favorable wear resistance under boundary lubricant conditions. Further analysis using SEM of the wear surfaces showed that a tribo-film formation was the primary wear reduction mechanism for WS_2 particles treated by PVP while, in the case of MoS_2, the mechanism was load sharing through particle rolling and/or sliding. Overall, the study demonstrates that stabilizing the dispersion of WS_2 and MoS_2 nanoparticles and minimizing agglomeration will improve wear resistance under boundary lubricant conditions.

Author Contributions: Conceptualization. Y.J. and S.S.; Methodology, Y.J. and T.L.; Investigation, Y.J., T.L., S.P.; Resources, S.P. and S.S.; Writing-Original Draft Preparation and Visualization, Y.J., T.L.; Writing-Review & Editing, S.S. and S.P.; Project Administration and Funding Acquisition, S.S.

Funding: This research was partial funded by the John Deere Product Engineering Center in Waterloo, Iowa (grant No. 125885) and Iowa State University.

Acknowledgments: The authors would like to thank Warren Straszheim from Material Characterization Research Laboratory for his collaboration in material characterization. Yosef Jazaa acknowledges scholarship support provided by Jazan University, Saudi Arabia.

Conflicts of Interest: The authors declare no conflict of interest.

References

1. Asrul, M.; Zulkifli, N.W.M.; Masjuki, H.H.; Kalam, M.A. Tribological properties and lubricant mechanism of nanoparticle in engine oil. *Procedia Eng.* **2013**, *68*, 320–325. [CrossRef]
2. Venkataraman, M. The Effect of Colloidal Stability on the Heat Transfer Characteristics of Nanosilica Dispersed Fluids. Master's Thesis, University of Central Florida, Orlando, FL, USA, 2005; p. 93.
3. Hwang, Y.; Lee, J.; Lee, J.; Jeong, Y.; Cheong, S.; Ahn, Y.; Kim, S.H. Production and dispersion stability of nanoparticles in nanofluids. *Powder Technol.* **2008**, *186*, 145–153. [CrossRef]
4. Zhang, W.; Zhou, M.; Zhu, H.; Tian, Y.; Wang, K.; Wei, J.; Ji, F.; Li, X.; Li, Z.; Zhang, P. Tribological properties of oleic acid-modified graphene as lubricant oil additives. *J. Phys. D Appl. Phys.* **2011**, *44*, 1–4. [CrossRef]
5. Rapoport, L.; Nepomnyashchy, O.; Lapsker, I.; Verdyan, A.; Soifer, Y.; Popovitz-Biro, R.; Tenne, R. Friction and wear of fullerene-like WS2 under severe contact conditions: Friction of ceramic materials. *Tribo. Lett.* **2005**, *19*, 143–149. [CrossRef]
6. Hansson, P.; Lindman, B. Surfactant-polymer interactions. *Curr. Opin. Colloid Interface Sci.* **1996**, *1*, 604–613. [CrossRef]
7. Feng, J.; Mao, J.; Wen, X.; Tu, M. Ultrasonic-assisted in situ synthesis and characterization of superparamagnetic Fe_3O_4 nanoparticles. *J Alloys Compd.* **2011**, *509*, 9093–9097. [CrossRef]
8. Chen, X.; Boulos, R.A.; Eggers, P.K.; Raston, C.L. *p*-Phosphonic acid calix[8]arene assisted exfoliation and Stabilization of 2D materials in water. *Chem. Commun.* **2012**, *48*, 11407–11409. [CrossRef]
9. Rao, Y. Particuology Nanofluids : Stability, phase diagram, rheology and applications. *Particuology* **2010**, *8*, 549–555. [CrossRef]

10. Ghadimi, A.; Metselaar, I.H. The influence of surfactant and ultrasonic processing on improvement of stability, thermal conductivity and viscosity of titania nanofluid. *Exp. Therm. Fluid Sci.* **2013**, *51*, 1–9. [CrossRef]
11. Kole, M.; Dey, T.K. Effect of aggregation on the viscosity of copper oxide-gear oil nanofluids. *Int. J. Therm. Sci.* **2011**, *50*, 1741–1747. [CrossRef]
12. Haddad, Z.; Abid, C.; Oztop, H.F.; Mataoui, A. A review on how the researchers prepare their nano fluids. *Int. J. Therm. Sci.* **2014**, *76*, 168–189. [CrossRef]
13. Kalin, M.; Kogovšek, J.; Remškar, M. Mechanisms and improvements in the friction and wear behavior using MoS 2 nanotubes as potential oil additives. *Wear* **2012**, *280–281*, 36–45. [CrossRef]
14. Chen, Z.; Liu, X.; Liu, Y.; Gunsel, S.; Luo, J. Ultrathin MoS_2 Nanosheets with Superior Extreme Pressure Property as Boundary Lubricants. *Sci. Rep.* **2015**, *5*, 12869. [CrossRef] [PubMed]
15. Lahouij, I.; Vacher, B.; Martin, J.M.; Dassenoy, F. IF-MoS_2 based lubricants: Influence of size, shape and crystal structure. *Wear* **2012**, *296*, 558–567. [CrossRef]
16. Abate, F.; D'Agostino, V.; Di Giuda, R.; Senatore, A. Tribological behaviour of MoS_2 and inorganic fullerene-like WS_2 nanoparticles under boundary and mixed lubrication regimes. *Tribol. Surf. Interfaces* **2010**, *4*, 91–98. [CrossRef]
17. Cizaire, L.; Vacher, B.; Le Mogne, T.; Martin, J.M.; Rapoport, L.; Margolin, A.; Tenne, R. Mechanisms of ultra-low friction by hollow inorganic fullerene-like MoS_2 nanoparticles. *Surf. Coat. Technol.* **2002**, *160*, 282–287. [CrossRef]
18. Yadgarov, L.; Petrone, V.; Rosentsveig, R.; Feldman, Y.; Tenne, R.; Senatore, A. Tribological studies of rhenium doped fullerene-like MoS_2 nanoparticles in boundary, mixed and elasto-hydrodynamic lubrication conditions. *Wear* **2013**, *297*, 1103–1110. [CrossRef]
19. An, V.; Irtegov, Y.; De Izarra, C. Study of tribological properties of nanolamellar WS_2 and MoS_2 as additives to lubricants. *Int. Nanomater.* **2014**, *2014*, 188.
20. Verma, A.; Jiang, W.; Abu Safe, H.H.; Brown, W.D.; Malshe, A.P. Tribological behavior of deagglomerated active inorganic nanoparticles for advanced lubrication. *Tribol. Trans.* **2008**, *51*, 673–678. [CrossRef]
21. Kedienhon, O. Characterization of Equilibrium Particle Size and Concentration in Oil-Based Nanolubricants. Master's Thesis, Department of Mechanical Engineering, Howard University, Washingtong, DC, USA, 2012.
22. Bari, R.; Parviz, D.; Khabaz, F.; Klaassen, C.D.; Metzler, S.D.; Hansen, M.J.; Khare, R.; Green, M.J. Liquid phase exfoliation and crumpling of inorganic nanosheets. *Phys. Chem. Chem. Phys.* **2015**, *17*, 9383–9393. [CrossRef]
23. Guardia, L.; Paredes, J.I.; Rozada, R.; Villar-Rodil, S.; Martínez-Alonso, A.; Tascón, J.M.D. Production of aqueous dispersions of inorganic graphene analogues by exfoliation and stabilization with non-ionic surfactants. *RSC Adv.* **2014**, *4*, 14115–14127. [CrossRef]
24. Moshkovith, A.; Perfiliev, V.; Lapsker, I.; Fleischer, N.; Tenne, R.; Rapoport, L. Friction of fullerene-like WS2 nanoparticles: Effect of agglomeration. *Tribol. Lett.* **2006**, *24*, 225–228. [CrossRef]
25. Aldana, P.U.; Dassenoy, F.; Vacher, B.; Le Mogne, T.; Thiebaut, B. WS2 nanoparticles anti-wear and friction reducing properties on rough surfaces in the presence of ZDDP additive. *Tribol. Int.* **2016**, *102*, 213–221. [CrossRef]
26. Joly-Pottuz, L.; Dassenoy, F.; Belin, M.; Vacher, B.; Martin, J.M.; Fleischer, N. Ultralow-friction and wear properties of IF-WS_2 under boundary lubrication. *Tribol. Lett.* **2005**, *18*, 477–485. [CrossRef]
27. Moshkovith, A.; Perfiliev, V.; Verdyan, A.; Lapsker, I.; Popovitz-Biro, R.; Tenne, R.; Rapoporta, L. Sedimentation of IF-WS_2 aggregates and a reproducibility of the tribological data. *Tribol. Int.* **2007**, *40*, 117–124. [CrossRef]
28. Ratoi, M.; Niste, V.B.; Walker, J.; Zekonyte, J. Mechanism of action of WS_2 lubricant nanoadditives in high-pressure contacts. *Tribol. Lett.* **2013**, *52*, 81–91. [CrossRef]
29. Zhang, X.; Xu, H.; Wang, J.; Ye, X.; Lei, W.; Xue, M.; Tang, H.; Li, C. Synthesis of Ultrathin WS_2 Nanosheets and Their Tribological Properties as Lubricant Additives. *Nanoscale Res. Lett.* **2016**, *11*, 442. [CrossRef]
30. Bogdan, V. WS_2 Nanoparticles—Potential Replacement for ZDDP and Friction Modifier Additives. *RSC Adv.* **2014**, *4*, 21238–21245.
31. Raichman, D.; Strawser, D.A.; Lellouche, J.P. Covalent functionalization/polycarboxylation of tungsten disulfide inorganic nanotubes (INTs-WS_2). *Nano Res.* **2014**, *8*, 1454–1463. [CrossRef]

32. Haba, D.; Griesser, T.; Müller, U.; Brunner, A.J. Comparative investigation of different silane surface functionalizations of fullerene-like WS_2. *J. Mater. Sci.* **2015**, *50*, 5125–5135. [CrossRef]
33. Liu, G.; Komatsu, N. Readily Available "Stock Solid" of MoS_2 and WS_2 Nanosheets through Solid-Phase Exfoliation for Highly Concentrated Dispersions in Water. *ChemNanoMat* **2016**, *2*, 500–503. [CrossRef]
34. Gulzar, M.; Masjuki, H.H.; Kalam, M.A.; Varman, M.; Mufti, R.A.; Zahid, R.; Yunus, R. AW/EP behavior of WS 2 nanoparticles added to vegetable oil—Based lubricant. In Proceedings of the Malaysian International Tribology Conference 2015, Penang, Malaysia, 16–17 November 2015; pp. 194–195.
35. Kamatchi, R.; Venkatachalapathy, S. Parametric study of pool boiling heat transfer with nanofluids for the enhancement of critical heat flux: A review. *Int. J. Therm. Sci.* **2015**, *87*, 228–240. [CrossRef]
36. Koczkur, K.M.; Mourdikoudis, S.; Polavarapu, L.; Skrabalak, S.E. Polyvinylpyrrolidone (PVP) in nanoparticle synthesis. *Dalton Trans* **2015**, *44*, 17883–17905. [CrossRef] [PubMed]
37. Fissan, H.; Ristig, S.; Kaminski, H.; Asbach, C.; Epple, M. Comparison of different characterization methods for nanoparticle dispersions before and after aerosolization. *Anal. Methods* **2014**, *6*, 7324–7334. [CrossRef]
38. Yella, A.; Tahir, M.N.; Meuer, S.; Zentel, R.; Berger, R.; Panthöfer, M.; Tremel, W. Synthesis, characterization, and hierarchical organization of tungsten oxide nanorods: Spreading driven by Marangoni flow. *J. Am. Chem. Soc.* **2009**, *131*, 17566–17575. [CrossRef]
39. Kole, M.; Dey, T.K. Role of interfacial layer and clustering on the effective thermal conductivity of CuO-gear oil nanofluids. *Exp. Therm. Fluid Sci.* **2011**, *35*, 1490–1495. [CrossRef]
40. Zhang, J.; Wang, Q.; Wang, L.; Li, X.; Huang, W. Layer-controllable WS2-reduced graphene oxide hybrid nanosheets with high electrocatalytic activity for hydrogen evolution. *Nanoscale* **2015**, *7*, 10391–10397. [CrossRef]
41. Wu, Y.Y.; Tsui, W.C.; Liu, T.C. Experimental analysis of tribological properties of lubricating oils with nanoparticle additives. *Wear* **2007**, *262*, 819–825. [CrossRef]
42. Zhang, L.; Liu, G.; Yang, G.B; Chen, S.; Huang, B.Y.; Zhang, C.F. Surface adsorption phenomenon during the preparation process of nano WC and ultrafine cemented carbide. *Int. J. Refract. Met. Hard Mater.* **2007**, *25*, 166–170. [CrossRef]
43. Xu, P.; Li, Z.; Zhang, X.; Yang, Z. Increased response to oxidative stress challenge of nano-copper-induced apoptosis in mesangial cells. *J. Nanoparticle Res.* **2014**, *16*. [CrossRef]
44. Rodriguez-Devecchis, V.M.; Carbognani Ortega, L.; Scott, C.E.; Pereira-Almao, P. Use of Nanoparticle Tracking Analysis for Particle Size Determination of Dispersed Catalyst in Bitumen and Heavy Oil Fractions. *Ind. Eng. Chem. Res.* **2015**, *54*, 9877–9886. [CrossRef]
45. Sonali, J.; Sandhyarani, N.; Sajith, V. Tribological properties and stabilization study of surfactant modified MoS_2 nanoparticle in 15W40 engine oil. *Int. J. Fluid Mech. Mach.* **2014**, *1*, 1–5.
46. Roy, S.; Sundararajan, S. The effect of heat treatment routes on the retained austenite and Tribomechanical properties of carburized AISI 8620 steel. *Surf. Coat. Technol.* **2016**, *308*, 236–243. [CrossRef]
47. Rabaso, P.; Ville, F.; Dassenoy, F.; Diaby, M.; Afanasiev, P.; Cavoret, J.; Vacher, B.; Le Mongne, T. Boundary lubrication: Influence of the size and structure of inorganic fullerene-like MoS2nanoparticles on friction and wear reduction. *Wear* **2014**, *320*, 161–178. [CrossRef]
48. Guo, D.; Xie, G.; Luo, J. Mechanical properties of nanoparticles: Basics and applications. *J. Phys. D Appl. Phys.* **2014**, *47*. [CrossRef]
49. Yang, G.B.; Chai, S.T.; Xiong, X.J.; Zhang, S.M.; Yu, L.G.; Zhang, P.Y. Preparation and tribological properties of surface modified Cu nanoparticles. *Trans. Nonferrous Met. Soc. China* **2012**, *22*, 366–372. [CrossRef]
50. Chiñas-Castillo, F.; Spikes, H.A. Mechanism of Action of Colloidal Solid Dispersions. *J. Tribol.* **2003**, *125*, 552–557. [CrossRef]